IEEE Journal of Translational Engineering in Health and Medicine

Received 30 August 2013; revised 8 November 2013; accepted 9 December 2013. Date of publication 9 January 2014; date of current version 24 January 2014.

Digital Object Identifier 10.1109/JTEHM.2014.2298852

Gastric Contraction Imaging System Using a 3-D Endoscope

KAYO YOSHIMOTO[1], KENJI YAMADA[1] (Member, IEEE), KENJI WATABE[2], MAKI TAKEDA[1], TAKAHIRO NISHIMURA[1], MICHIKO KIDO[1], TOSHIAKI NAGAKURA[3] (Member, IEEE), HIDEYA TAKAHASHI, TSUTOMU NISHIDA[2], HIDEKI IIJIMA[2], MASAHIKO TSUJII[2], TETSUO TAKEHARA[2], AND YUKO OHNO[1]

[1]Division of Health Sciences, Graduate School of Medicine, Osaka University, Osaka 565-0871, Japan
[2]Department of Gastroenterology and Hepatology, Graduate School of Medicine, Osaka University, Osaka 565-0871, Japan
[3]Department of Biomedical Engineering, Graduate School of Biomedical Engineering, Osaka Electro-Communication University, Osaka 575-0063, Japan

Corresponding Author: K. YOSHIMOTO (k-yoshi@sahs.med.osaka-u.ac.jp)

This work was supported by JSPS KAKENHI under Grant 24500546.

ABSTRACT This paper presents a gastric contraction imaging system for assessment of gastric motility using a 3-D endoscope. Gastrointestinal diseases are mainly based on morphological abnormalities. However, gastrointestinal symptoms are sometimes apparent without visible abnormalities. One of the major factors for these diseases is abnormal gastrointestinal motility. For assessment of gastric motility, a gastric motility imaging system is needed. To assess the dynamic motility of the stomach, the proposed system measures 3-D gastric contractions derived from a 3-D profile of the stomach wall obtained with a developed 3-D endoscope. After obtaining contraction waves, their frequency, amplitude, and speed of propagation can be calculated using a Gaussian function. The proposed system was evaluated for 3-D measurements of several objects with known geometries. The results showed that the surface profiles could be obtained with an error of $<$10% of the distance between two different points on images. Subsequently, we evaluated the validity of a prototype system using a wave simulated model. In the experiment, the amplitude and position of waves could be measured with 1-mm accuracy. The present results suggest that the proposed system can measure the speed and amplitude of contractions. This system has low invasiveness and can assess the motility of the stomach wall directly in a 3-D manner. Our method can be used for examination of gastric morphological and functional abnormalities.

INDEX TERMS Endoscopes, gastric contraction, gastric motility, gastroenterology.

I. INTRODUCTION

Functional gastrointestinal disorders (e.g., functional dyspepsia and irritable bowel syndrome) are frequent conditions encountered in clinical practice [1], [2]. According to a recent systematic review and meta-analysis, the prevalence of functional dyspepsia was 27% and that of irritable bowel syndrome was 16% [3]. People with functional gastrointestinal disorders experience gastrointestinal symptoms despite the absence of morphological or anatomical abnormalities. While these disorders are not life-threatening, it was noted that quality of life was markedly impaired and productivity was decreased in such patients [4]–[6]. One of the major factors for these diseases is abnormal gastric motility. The principal functions of the stomach are reservoir, mixing, and emptying of gastric contents. The fundus acts as the reservoir, and the gastric corpus and gastric antrum facilitate mixing and emptying. Contraction and dilatation of the stomach are related to these functions, and abnormal gastric motility leads to depression of these functions. For functional assessment of gastrointestinal motility, the barostat technique is the current standard [7], [8]. This system estimates the gastric tone by the change in volume or pressure of air in a balloon placed in a hollow organ. However, the burden on the patient is large. Scintigraphy and ^{13}C breath tests are also important methods [9]–[11]. These methods track the motion of a marker, included in a meal, from outside of the body. Although these methods are non-invasive, they involve indirect assessment of gastric motility, because the system can only assess the gastric flow produced by the gastric motility. Magnetic resonance imaging (MRI) has been used to investigate dynamic gastrointestinal motility [12]–[16]. MRI can obtain the whole shape of the stomach, including the motility. It can estimate the volume of the stomach or detect gastric contraction waves generated for the mixing and emptying functions by measuring the stomach shape. It has been elucidated that gastric contraction waves are different in healthy humans and patients with functional gastrointestinal disorders through the use of MRI [15], [16]. However, this system can only obtain two-dimensional cross-sectional images of the stomach. Therefore, functional quantitative analyses by MRI would be untrue.

On the other hand, an endoscope can be used to look inside the body, including observation of the gastrointestinal tract. For such examinations, endoscopes are mainly used to detect organic abnormalities. Recently, three-dimensional endoscopes have been developed and put into practical use [17]–[20]. A three-dimensional endoscope is currently almost always used as a surgical navigation system. However, it is expected that they will become useful as diagnostic instruments, because it is possible to obtain the three-dimensional shape of an organ from inside of the body.

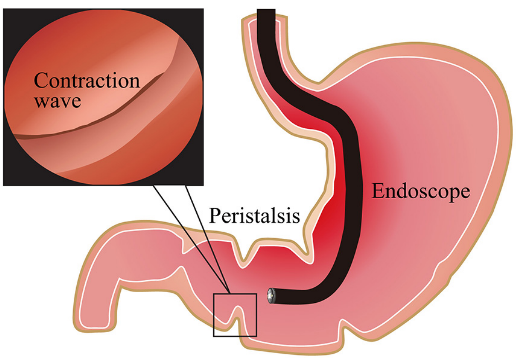

FIGURE 1. **Modality of the stomach.**

This paper presents a gastric contraction imaging system using an endoscope, as shown in Fig. 1. By using the three-dimensional shape of the stomach obtained from the endoscope, contraction waves are measured to assess the gastric motility. This system has low invasiveness and can assess the motility of the stomach wall directly in a three-dimensional manner. In addition, an endoscope is usually used for examination of the stomach. In other words, no additional equipment is required for assessment of the motility.

In this paper, we evaluate the proposed gastric motility imaging system using a three-dimensional endoscope. In section II, we introduce a method for assessing gastric motility. In section III, we evaluate the performance of a prototype three-dimensional endoscope and the effectiveness of the proposed method in an experiment with a wave simulated model. Finally, we provide some conclusions in Section V.

II. WAVE MEASUREMENT SYSTEM

A. THREE-DIMENSIONAL ENDOSCOPE

For three-dimensional measurements, the proposed system employs a compound eye system. We previously developed a compound eye system called the TOMBO (Thin Observation Module by Bound Optics) [21]–[23]. This system has a compact structure and can take close images because it uses a micro-lens array. This feature is an advantage because the optical system involves a flexible endoscope that allows bending. Moreover, this system can simultaneously obtain multiple images with positional shifts. These images are available for use in wide-field, high-resolution, and three-dimensional measurements. The TOMBO is well suited for the three-dimensional endoscope.

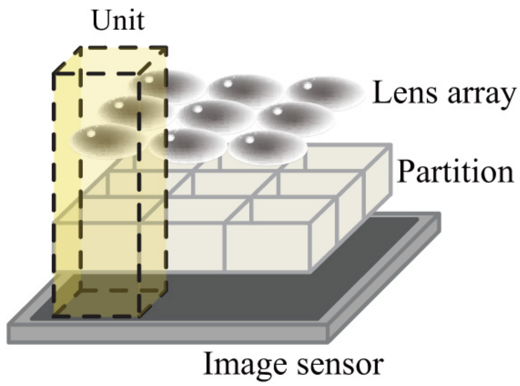

FIGURE 2. **Basic structure of the TOMBO.**

A schematic diagram of the compound optics system is shown in Fig. 2. The compound optics system consists of a micro-lens array, partition, and CMOS image sensor. Each micro-lens focuses optical signals on the image sensor. The images obtained by this system are presented with slightly different information for the view. Based on triangulation, three-dimensional information about the imaged object can be computed. An area-based method with the sum of the squared difference is used to obtain the corresponding points in two images. A sub-pixel estimation with a parabolic function and cross-checking by replacing the left and right images is also used to improve the accuracy of measurement. Searching for corresponding points for all pixels on one image, the three-dimensional profile of the object can be estimated.

B. DATA ANALYSIS

For analysis of gastric motility, gastric contractions are derived from the three-dimensional profile of the stomach wall. Gastric contractions propagate from the gastric corpus to the pylorus. The three-dimensional profile of the stomach is mixed with the stomach geometry itself and the contraction profile, as shown in Fig. 1. Therefore, the contraction waves must be separated from the three-dimensional profile of the stomach wall for analysis. The geometry of the stomach is obtained as the most frequent value in a time series, and the other value reflects the contraction profile. The shape of the contractions is obtained by measuring the distance between the geometry of the stomach and the measurement profiles. The three-dimensional data obtained from the three-dimensional endoscope include noise or outliers, and

IEEE Journal of Translational Engineering in Health and Medicine

missing areas caused by masking could exist. To overcome these problems, we model the geometry of the stomach and the contraction waves. Here, the shape of the gastric contractions is modeled by a one-dimensional Gaussian function [24] and the geometry of the gastric antrum is regarded as a circular tube, as shown in Fig. 3. The one-dimensional Gaussian function on the x-axis can be expressed as follows:

$$G(x) = Ne^{\left(-\frac{x-x_c}{2\sigma^2}\right)} \tag{1}$$

where N and x_c are the attitude and position of the wave, respectively, and σ indicates the spread of the wave. From the Gaussian parameters, the amplitude and speed of each contraction can be calculated.

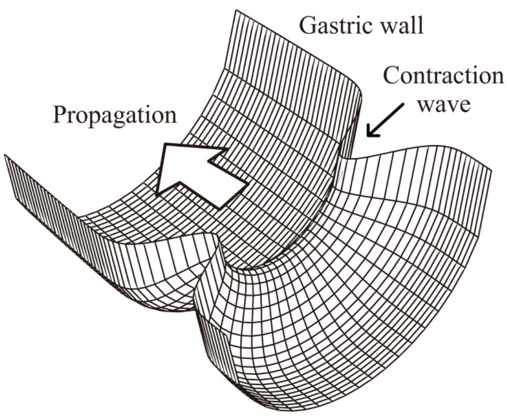

FIGURE 3. Geometry of the antrum with peristaltic contractions.

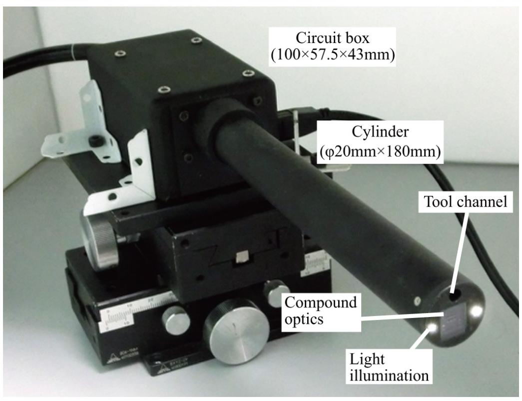

FIGURE 4. Photograph of the endoscope-type TOMBO.

III. EXPERIMENT

A. PROTOTYPE THREE-DIMENSIONAL ENDOSCOPE SYSTEM

Fig. 4 shows an overview of the prototype endoscope system. A custom-made rigid endoscope with a compound optics system was used to reconstruct three-dimensional images. The tip of the endoscope has a tool channel, compound optics, and illumination. Table 1 shows the specification of the prototype system. The imaging sensor used was AR0331 (Aptina Imaging Co.). The light source device used was CLV-U20D (Olympus Co.). In this study, we used two images arranged on the y-axis for three-dimensional measurements. The baseline length was approximately 2.2 mm. We defined a coordinate system for the endoscope as follows: z-axis parallel to the optical axis; and $x-$ and y-axes parallel to the image sensor. The experiment was conducted after calibration of the optics and stereo images.

TABLE 1. Specification of the prototype.

Lens array	3 × 3
Focal length	1.5 mm
F-number	7.5
Angle of field	46 degrees
Depth of field	20-50 mm
Pixel size	2.2 μm
Pixel count (per unit)	415 × 415

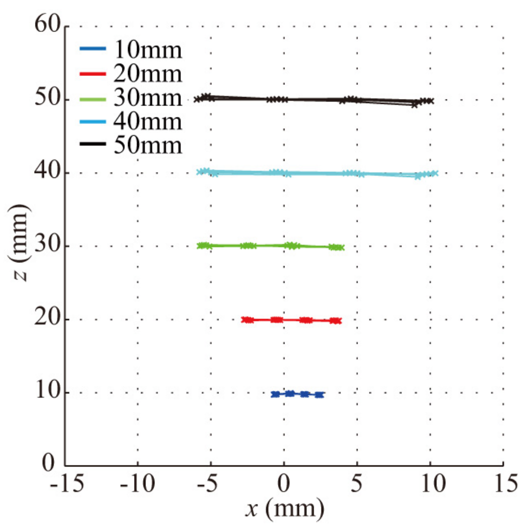

FIGURE 5. Reconstruction of the surface of a flat plane on the x–z plane at different distances from the endoscope tip.

B. ACCURACY EVALUATION FOR THREE-DIMENSIONAL MEASUREMENTS

First, we evaluated the accuracy of the three-dimensional measurements using the prototype system. A target with the simplest of geometric features was used to evaluate the accuracy of depth measurements. A rigid flat plane with a grid sheet was fixed on a one-dimensional translation stage. The distance between the endoscope tip and the target surface could be adjusted. The target plane size was 50 mm × 75 mm. The cross points of the grid were used as the features and the grid interval was 1 mm. Images of the grid on the target were taken at distances from the endoscope tip starting at 10 mm and finishing at 50 mm with 10-mm increments. A feature point was designated manually and the corresponding point was obtained automatically. Typical results are shown in Fig. 5. The means and standard deviations of the estimated distances from the target plane to the endoscope tip for the set distances of 10, 20, 30, 40, and 50 mm were 9.8 ± 0.066, 19.9 ± 0.061, 30.0 ± 0.121, 40.0 ± 0.198, and 50.0 ± 0.264 mm, respectively, in three trials for each distance. The percentage of measurement error for the distance between the endoscope tip and the target plane was less than 2% when the distance ranged from 10 to 50 mm.

In the second experiment, we evaluated the measurement accuracy for the distance between two different feature points. The target was fixed on a rotator that permitted the angle between the optical axis of the endoscope and the orientation of the flat plane to be changed. The distance of the rotation center from the endoscope tip was 30 mm. The angle between the flat plane and the optical axis was then changed in increments of 15 degrees up to 75 degrees. The means and standard deviations of the estimated distances between two different feature points separated by 1 mm for the set distances of 10, 20, 30, 40, and 50 mm were 1.01 ± 0.020, 1.01 ± 0.010, 1.01 ± 0.011, 1.00 ± 0.012, and 1.00 ± 0.009 mm, respectively. The means and standard deviations for the same points at the set angles of 15, 30, 45, 60, and 75 degrees were 1.01 ± 0.011, 1.01 ± 0.011, 1.01 ± 0.017, 1.01 ± 0.020, and 0.95 ± 0.081 mm, respectively. The percentage of measurement error for the distance between two different points was less than 6% when the distance ranged from 10 to 50 mm and the angle ranged from 15 to 60 degrees. For the angle of 75 degrees, the percentage of maximum measurement error was about 25%. This error could be caused by masking of the corresponding point.

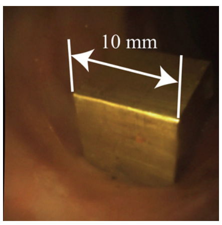

FIGURE 6. **Brass cube on the dog colon obtained by the prototype system.**

Finally, to evaluate the accuracy of the prototype system in the clinical situation, we conducted experiments with a dog. A 10-mm brass cube was put on the colon of the dog, as shown in Fig. 6. The length of the upper side of the cube was measured. The mean value for the measured length was 10.4 ± 0.35 mm in three pairs of images obtained from different positions. The measurement length was longer than the correct length in all cases. This error could be caused by secretory fluid attached to the cover glass of the lens.

C. MEASUREMENTS IN A WAVE SIMULATED MODEL

Next, we evaluated the validity of wave measurements using a wave simulated model. The object used for the wave simulated model was a plastic spring cylinder, as shown in Fig. 7. A wave was made on the spring's surface by pushing the coil from the opposite surface. The amplitude of the wave was approximately 7 mm. The wave was manually propagated with increments of approximately 3.2 mm along the central axis of the spring. In this case, the wave generated on the plane was mixed with the shape of the spring, and we thus used a rectangular coordinate system. We defined a coordinate system for the object as follows: Z-axis parallel to the contraction; X-axis parallel to the central axis of the spring; and Y-axis parallel to another axis. The geometry of the cylinder itself was measured by obtaining images without waves. We then approximated the geometry by the paraboloidal surface. The parameter of the paraboloid was used for axial correction. After axial correction, the shape of the waves could be obtained by subtracting the paraboloidal surface and the reconstructed shape of the surface along the Z-axis.

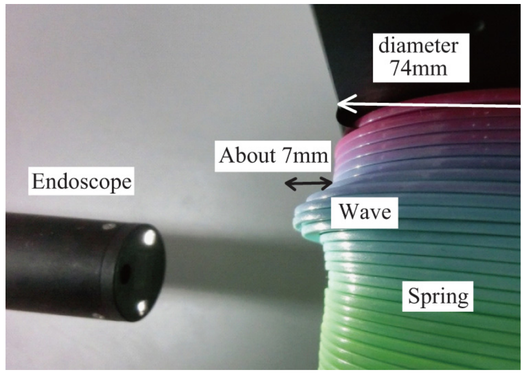

FIGURE 7. **Experimental setup for measurements in the wave simulated model.**

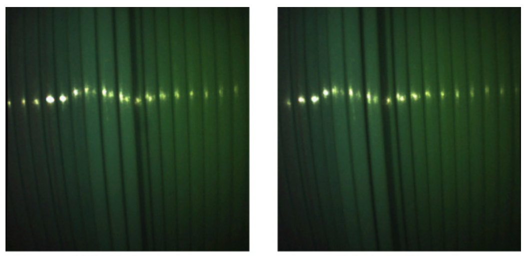

FIGURE 8. **Images obtained by the endoscope. (a) Left image. (b) Right image.**

The object was placed so that the vibration direction of the wave was along the z-axis and the central axis of the spring was along the x-axis. Fig. 8 shows one of the captured images of a wave made on the spring surface. The reconstructed shape of the spring surface is shown in Fig. 9. Fig. 10 shows the extracted contraction wave. The attitude of the wave was 7.1 mm. Fig. 11 shows the position and attitude of the detected wave when the wave was propagated in increments of about +3.2 mm along the central axis of the spring (X-axis). In Fig. 11, S_i (i = 1, 2, ...) means the surface that propagated the wave by +3.2 mm from S_{i-1}. The mean measured value for the attitude was 7.2 ± 0.3 mm. The mean measured value for the wave movement along the X-axis was about +3.2 mm.

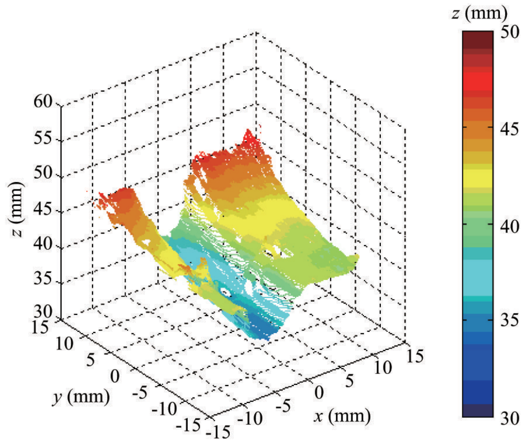

FIGURE 9. Reconstructed shape of the spring surface.

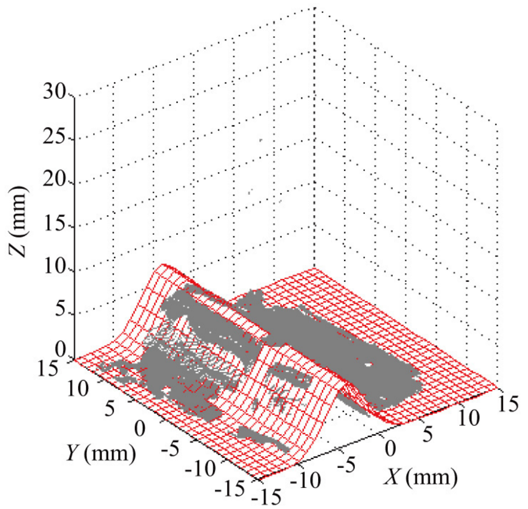

FIGURE 10. Extracted wave of the spring surface. Gray dots show the raw data and red lines show the Gaussian function-fitted raw data.

Next, to evaluate the potential for clinical application, the wave simulated model was covered with thinly-sliced pork. Fig. 12 shows one of the captured images of a wave made on the pork surface. The reconstructed shape of the pork surface is shown in Fig. 13. The attitude of the wave was 6.4 mm. The mean measured value for the attitude was 6.6 ± 0.3 mm and the mean measured value for the wave movement was about +3.3 mm, as shown in Fig. 14.

In the same way, Fig. 15 shows typical results for an angle of 30 degrees between the central axis of the spring and the optical axis. Fig. 16 shows the position and attitude of the detected wave in the coordinates of the wave when the wave was manually propagated with increments of about +3.2 mm along the X-axis. The mean measured value for the attitude

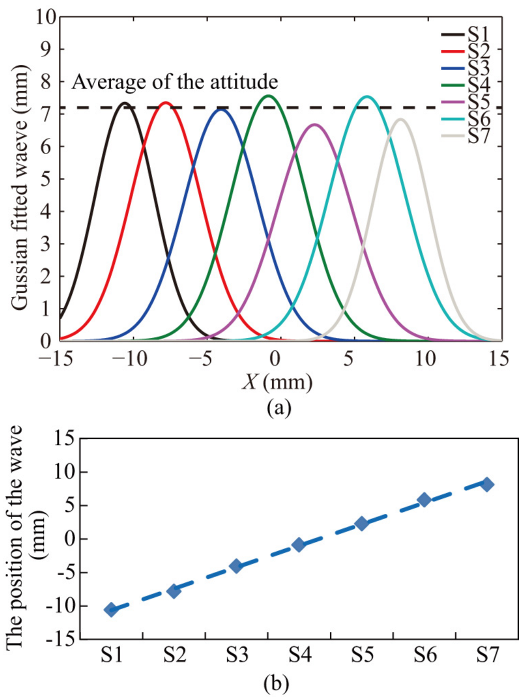

FIGURE 11. Detected propagated waves extracted from the spring surface. (a) Gaussian function-fitted wave and (b) position of the wave. The average wave attitude is 7.2 mm and the average wave movement is +3.3 mm.

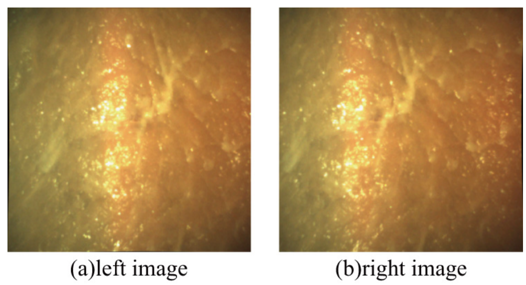

FIGURE 12. Images obtained by the endoscope. The object is covered with thinly-sliced pork. (a) Left image. (b) Right image.

was 6.1 ± 0.3 mm. The mean measured value for the wave movement along the X-axis was about +3.0 mm.

IV. DISCUSSION

We have demonstrated a three-dimensional endoscope system for assessment of gastrointestinal motility. First, we evaluated the performance of a prototype endoscope system. The prototype system could measure the geometry of a flat plane with an error of less than 10 percent of the distance between two different points on images. Subsequently, we conducted experiments with a dog to evaluate the accuracy of the prototype system for a clinical status using an object with known geometry. These results suggested that our system could achieve quantitative measurements for a clinical status. However, some errors occurred in the animal experiment, which were caused by secretory fluid. A secreted fluid

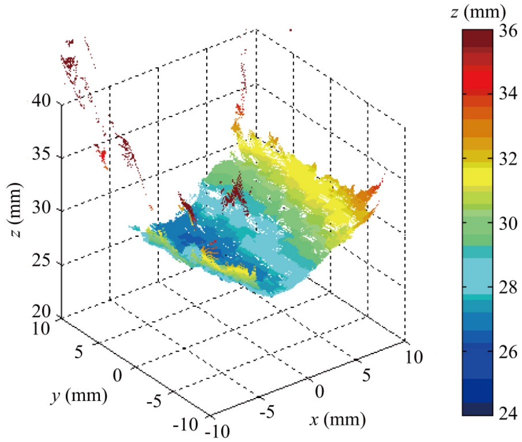

FIGURE 13. Reconstructed shape of the pork surface.

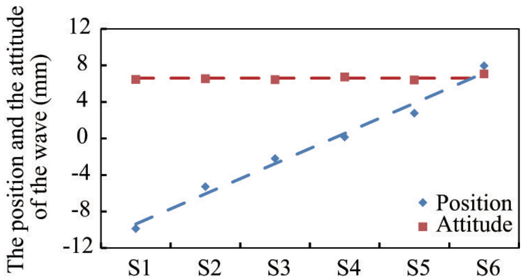

FIGURE 14. Position and attitude of detected propagated waves extracted from the pork surface.

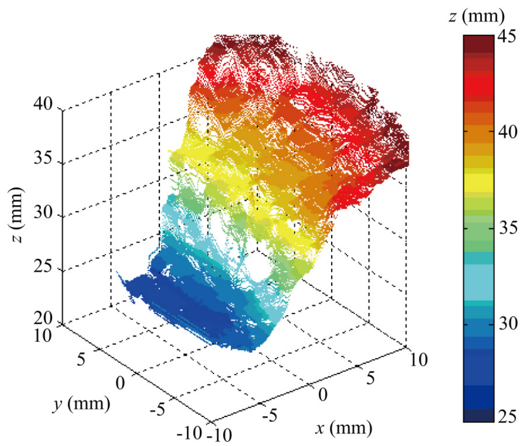

FIGURE 15. Reconstructed shape of the pork surface with an angle of 30 degrees between the cylinder axis and the optical axis.

is an obstacle for measurement, and a matching error occurs because the image is blurred by water droplets. Since our system does not have equipment to remove any dirt present, the secretory fluid attached to the cover glass of the lens cannot be removed. A water supply nozzle function is needed for stable measurements.

Next, we demonstrated a three-dimensional endoscope system for assessment of gastrointestinal motility using a wave simulated model. The experimental results showed that the

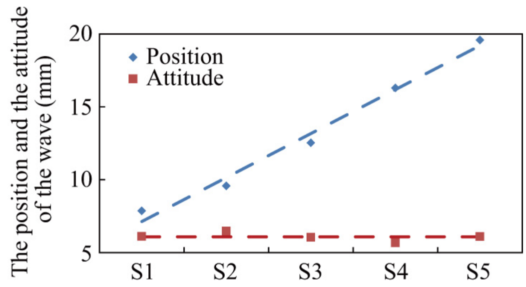

FIGURE 16. Position and attitude of detected propagated waves extracted from the pork surface with an angle of 30 degrees between the cylinder axis and the optical axis.

amplitude and position of a wave could be measured with 1-mm accuracy. Unlike MRI, an endoscope cannot capture the whole shape of the stomach at once. The hidden surface of the contraction wave cannot be used to reconstruct the three-dimensional profile. Thus, the proposed system estimates the shape of peristaltic contractions through the use of a one-dimensional Gaussian function. Nevertheless, the wave surface opposite to the endoscope had low information when the angle between the central axis of the object and the optical axis was 30 degrees, and the estimated surface fitted by the Gaussian function was quite well fitted with the raw data. From the data shown in Figs. 14 and 16, the estimated attitudes of the waves were almost constant. These results suggest that the prototype system can provide measurements with high robustness.

Kwiatek et al. [15] and Pal et al. [16] measured the details of peristaltic contractions in healthy volunteers using MRI. Contraction waves were initiated every 20 s, and the width and speed of these waves were 18 mm and 2.5 mm/s, respectively. The amplitude of the waves was 7 mm. These parameters are similar to those in the wave simulated model. The prototype system obtains 4 frames/s. The speed of the contraction wave is sufficiently slower than the performance of the prototype system. Consequently, the prototype system can detect contraction waves of the stomach.

In a clinical status, it is hardly possible for operators to keep the tip immobile. Thus, the obtained images are recorded from different viewing positions in a time series and the contraction waves on images also move with the movement of the endoscope tip. This issue can be solved by performing three-dimensional registration [25] using a portion that does not move, because contraction waves are sufficiently slower than the movement of the endoscope and occur partially. This is part of our future work.

V. CONCLUSION

In this paper, we have proposed a gastric contraction imaging system for assessment of gastric motility using a three-dimensional endoscope. For analysis of gastric motility, we described a method that derived peristaltic contractions from the three-dimensional profile of the stomach wall. Moreover, we evaluated the developed three-dimensional endoscope system using a flat plane. This system can measure the geometry of a flat plane with an error of less than 10 percent of the distance between two different points on images. Subsequently, we conducted experiments with a dog to evaluate the accuracy of the prototype system for a clinical status using an object with known geometry. These results suggested that our system could achieve quantitative measurements for a clinical status. We then evaluated the validity of a prototype system using a wave simulated model. In that experiment, we demonstrated that the amplitude and position of the wave can be measured with 1-mm accuracy. These results suggest that the proposed system can measure the speed and amplitude of contractions. In the future, we will evaluate the proposed system using in vivo experiments.

ACKNOWLEDGMENT

The authors would like to thank KONICA MINOLTA Inc. for supporting the development of the prototype system.

REFERENCES

[1] J. Tack, N. J. Talley, M. Camilleri, G. Holtmann, P. Hu, J.-R. Malagelada, *et al.*, "Functional gastroduodenal disorders," *Gastroenterology*, vol. 130, no. 5, pp. 1466–1479, 2006.

[2] J. Hyams, "Functional gastrointestinal disorders," *Current Opinion Pediatrics*, vol. 11, no. 5, pp. 375–378, 1999.

[3] A. C. Ford, A. Marwaha, A. Lim, and P. Moayyedi, "Systematic review and meta-analysis of the prevalence of irritable bowel syndrome in individuals with dyspepsia," *Clin. Gastroenterol. Hepatol.*, vol. 8, no. 5, pp. 401–409, 2010.

[4] S. L. S. Halder, G. R. Locke, N. J. Talley, S. L. Fett, A. R. Zinsmeister, and L. J. Melton, "Impact of functional gastrointestinal disorders on health-related quality of life: A population-based case-control study," *Alimentary Pharmacol. Therapeutics*, vol. 19, no. 2, pp. 233–242, 2004.

[5] M. Kaji, Y. Fujiwara, M. Shiba, Y. Kohata, H. Yamagami, T. Tanigawa, *et al.*, "Prevalence of overlaps between GERD, FD and IBS and impact on health-related quality of life," *J. Gastroenterol. Hepatol.*, vol. 25, no. 6, pp. 1151–1156, 2010.

[6] R. A. Brook, N. L. Kleinman, R. S. Choung, A. K. Melkonian, J. E. Smeeding, and N. J. Talley, "Functional dyspepsia impacts absenteeism and direct and indirect costs," *Clin. Gastroenterol. Hepatol.*, vol. 8, no. 6, pp. 498–503, 2010.

[7] F. Azpiroz and J. R. Malagelada, "Physiological variations in canine gastric tone measured by an electronic barostat," *Amer. J. Physiol.*, vol. 248, no. 2, pp. G229–G237, 1985.

[8] K. A. Undeland, T. Hausken, O. H. Gilja, R. Ropert, J. P. Galmiche, and A. Berstad, "Gastric relaxation in response to a soup meal in healthy subjects. A study using a barostat in the proximal stomach," *Scandin. J. Gastroenterol.*, vol. 30, no. 11, pp. 1069–1076, 1995.

[9] B. Pfaffenbach, R. J. Adamek, C. B. Aus, and M. Wegener, "Gastric dysrhythmias and delayed gastric emptying in patients with functional dyspepsia," *Dig. Diseases Sci.*, vol. 42, no. 10, pp. 2094–2099, 1997.

[10] H. P. Parkman, M. A. Miller, D. Trate, L. C. Knight, J. L. Urbain, A. H. Maurer, *et al.*, "Electrogastrography and gastric emptying scintigraphy are complementary for assessment of dyspepsia," *J. Clin. Gastroenterol.*, vol. 24, no. 4, pp. 214–219, 1997.

[11] J. Punkkinen, I. Konkka, O. Punkkinen, T. Korppi-Tommola, M. Färkkilä, and J. Koskenpato, "Measuring gastric emptying: Comparison of 13C-octanoic acid breath test and scintigraphy," *Dig. Diseases Sci.*, vol. 51, no. 2, pp. 262–267, 2006.

[12] P. Kunz, C. Feinle, W. Schwizer, M. Fried, and P. Boesiger, "Assessment of gastric motor function during the emptying of solid and liquid meals in humans by MRI," *J. Magn. Reson. Imag.*, vol. 9, no. 1, pp. 75–80, 1999.

[13] W. Ajaj, S. C. Goehde, N. Papanikolaou, G. Holtmann, S. G. Ruehm, J. F. Debatin, *et al.*, "Real time high resolution magnetic resonance imaging for the assessment of gastric motility disorders," *Gut*, vol. 53, no. 9, pp. 1256–1261, 2004.

[14] S. Bickelhaupt, J. M. Froehlich, R. Cattin, S. Raible, H. Bouquet, U. Bill, *et al.*, "Software-supported evaluation of gastric motility in MRI: A feasibility study," *J. Med. Imag. Radiat. Oncol.*, Jul. 2013, doi: 10.1111/1754-9485.12097.

[15] M. Kwiatek, A. Steingoetter, A. Pal, D. Menne, J. G. Brasseur, G. S. Hebbard, *et al.*, "Quantification of distal antral contractile motility in healthy human stomach with magnetic resonance imaging," *J. Magn. Reson. Imag.*, vol. 24, no. 5, pp. 1101–1009, 2006.

[16] A. Pal, K. Indireshkumar, W. Schwizer, B. Abrahamsson, M. Fried, and J. G. Brasseur, "Gastric flow and mixing studied using computer simulation," *Proc. R. Soc. B, Biol. Sci.*, vol. 271, no. 1557, pp. 2587–2594, 2004.

[17] G. B. Hanna, S. M. Shimi, and A. Cuschieri, "Randomised study of influence of two-dimensional versus three-dimensional imaging on performance of laparoscopic cholecystectomy," *Lancet*, vol. 351, no. 9098, pp. 248–51, 1998.

[18] A. Tabaee, V. K. Anand, J. F. Fraser, S. M. Brown, A. Singh, and T. H. Schwartz, "Three-dimensional endoscopic pituitary surgery," *Neurosurgery*, vol. 64, no. 5, pp. 288–293, 2009.

[19] M. Chan, W. Lin, C. Zhou, and J. Y. Qu, "Miniaturized three-dimensional endoscopic imaging system based on active stereovision," *Appl. Opt.*, vol. 42, no. 10, pp. 1888–1898, 2003.

[20] K. Kihara, Y. Fujii, H. Masuda, K. Saito, F. Koga, Y. Matsuoka, *et al.*, "New three-dimensional head-mounted display system, TMDU-S-3D system, for minimally invasive surgery application: Procedures for gasless single-port radical nephrectomy," *Int. J. Urol.*, vol. 19, no. 9, pp. 886–889, 2012.

[21] J. Tanida, T. Kumagai, K. Yamada, S. Miyatake, K. Ishida, T. Morimoto, *et al.*, "Thin observation module by bound optics (TOMBO): Concept and experimental verification," *Appl. Opt.*, vol. 40, no. 11, pp. 1806–1013, 2001.

[22] K. Yamada and H. Takahashi, "Evaluation of three-dimensional endoscope using compound eye optical system with multi-wavelength band-pass filter," *IJICIC*, vol. 7, no. 8, pp. 4691–4701, 2011.

[23] K. Kagawa, K. Yamada, E. Tanaka, and J. Tanida, "A three-dimensional multifunctional compound-eye endoscopic system with extended depth of field," *Electron. Commun. Jpn.*, vol. 95, no. 11, pp. 14–27, 2012.

[24] Y. Imai, I. Kobayashi, S. Ishida, T. Ishikawa, M. Buist, and T. Yamaguchi, "Antral recirculation in the stomach during gastric mixing," *Amer. J. Physiol. Gastrointestinal Liver Physiol.*, vol. 304, no. 5, pp. G536–G542, 2013.

[25] S. Rusinkiewicz and M. Levoy, "Efficient variants of the ICP algorithm," in *Proc. 3rd Int. Conf. 3-D Digital Imag. Model.*, 2001, pp. 145–152, .

KAYO YOSHIMOTO received the B.E. and M.E. degrees in mechanical engineering from Osaka University, Osaka, Japan, in 2009 and 2011, respectively, where she is currently pursuing the Ph.D. degree with the Graduate School of Medicine. Her current research interests include medical engineering and nursing engineering.

KENJI YAMADA received the Doctoral degree from the Graduate School of Engineering, Osaka City University in 1998. He became an Associate Professor with the Hiroshima Institute of Technology. After serving as an Associate Professor with the Center for Advanced Medical Engineering and Informatics, Osaka University, he has been a Professor with the Graduate School of Medicine, Osaka University, since 2012. His research interests are optical information processing, medical engineering, 3-D measurement, and micromachining. He is now engaged in research on nursing engineering. He is a member of JSMBE, SICE, SPIE, and other societies.

KENJI WATABE is an Assistant Professor with the Graduate School of Medicine, Osaka University, Osaka, Japan. He received the M.D. and Ph.D. degrees from Osaka University in 1994 and 2001, respectively. He was a Post-Doctoral Fellow with the Graduate School of Frontier Biosciences, Osaka University, from 2002 to 2004.

His research interests include the field of gastroenterology, especially gastroenterological diseases and interstitial cells of Cajal.

MAKI TAKEDA received the Doctoral degree from the Graduate School of Medicine, Osaka University, in 2013.

She has been a Project Researcher with Osaka University since 2013. Her research interests are cancer, medical engineering, and nursing engineering.

TAKAHIRO NISHIMURA is a Post-Doctoral Researcher with Osaka University. He received the B.S. degree in applied physics and the M.S. and Ph.D. degrees in information science from Osaka University in 2008, 2010, and 2013, respectively.

His current research interests include information photonics and biomedical engineering.

MICHIKO KIDO received the master's degree from the Graduate School of Nursing, Osaka University, in 2011. She was a Nurse and Chief Nurse with the National Hospital Organization. She has been an Assistant Professor with the Graduate School of Medicine, Osaka University, since 2013. Her research interests include clinical nursing study. She is now engaged in research on nursing health assessment and nursing management.

TOSHIAKI NAGAKURA received the M.D. degree from Osaka University in 1990. He was a Research Fellow of cardiology with the First Department of Medicine, Osaka University Medical School, from 1991 to 1997. After serving as an Associate Professor with the Suzuka University of Medical Science, he has been a Professor with Osaka Electro-Communication University since 2002. His research interests are medical engineering, MEMS, endoscope, 3-D measurement, image processing, medical informatics, and medical design. He is a member of JSMBE, JAMI, JSCAS, JSSD, and other societies.

HIDEYA TAKAHASHI received the B.E., M.E., and Ph.D. degrees in electrical engineering from Osaka City University in 1982, 1984, and 1992, respectively. Since 1987, he has been a Faculty Member with Osaka City University, and since 2011, he has been a Professor with the Department of Electric and Information Engineering. His current research interests include interactive 3-D display, retinal projection display, wearable computers, and medical engineering. He is a member of SPIE and OSA.

TSUTOMU NISHIDA was born in Oita, Japan, in 1969. He received the Medical License and Ph.D. degrees in medicine from the Graduate School of Medicine, Osaka University, in 1994 and 2006, respectively. Since 2006, he has been with Osaka University Hospital as a Gastroenterologist. His research interests include gastrointestinal oncology and endoscopy. Dr. Nishida is an Assistant Professor of gastroenterology and hepatology with the Graduate School of Medicine, Osaka University.

HIDEKI IIJIMA is an Assistant Professor with the Graduate School of Medicine, Osaka University, Osaka, Japan. He received the M.D. and Ph.D. degrees from Osaka University in 1990 and 1999, respectively. He was a Post-Doctoral Fellow with the Division of Gastroenterology, Brigham and Women's Hospital, Harvard Medical School, Boston, MA, USA, from 2000 to 2002. His research interests include the field of gastroenterology, especially inflammatory bowel disease and mucosal immunology.

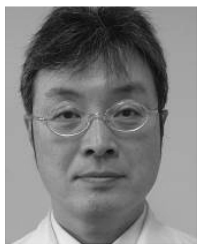

MASAHIKO TSUJII is an Associate Professor with the Graduate School of Medicine, Osaka University, Osaka, Japan. He received the M.D. and Ph.D. degrees from Osaka University in 1984 and 1992, respectively. He was a Post-Doctoral Fellow with the Division of Cell Biology, Vanderbilt University, Nashville, TN, USA, from 1993 to 1995. His research interests include the field of gastroenterology, especially oncology and immunology in gastrointestinal cancer and inflammatory bowel disease.

TETSUO TAKEHARA is a Professor with the Graduate School of Medicine, Osaka University, Osaka, Japan. He received the M.D. and Ph.D. degrees from Osaka University in 1984 and 1993, respectively. He was a Research Fellow with Massachusetts General Hospital GI Unit, Boston, MA, USA. His research interests include cell death, innate immunity, viral hepatitis, and hepatocellular carcinoma.

YUKO OHNO received the Ph.D. degree in medical engineering from the University of Tokyo, Tokyo, Japan, in 1985. She became a Research Fellow with the National Institute of Statistical Mathematics. After serving as a Senior Researcher with the Tokyo Metropolitan Institute for Neuroscience, she has been a Professor with the Graduate School of Medicine, Osaka University, Osaka, Japan, since 1995. Her research interests include mathematical health science, operation metrics, robotics and design for innovative healthcare, and phenomenal design.